Enzyme-modified nanoporous gold-based electrochemical biosensors

Huajun Qiu[a], Luyan Xue[a], Guanglei Ji[a], Guiping Zhou[a], Xirong Huang[a,*], Yinbo Qu[b], Peiji Gao[b]

[a] Key Laboratory of Colloid and Interface Chemistry of the Ministry of Education of China, Shandong University, No. 27 Shanda Nalu, Jinan 250100, China
[b] State Key Laboratory of Microbial Technology of China, Shandong University, Jinan, China

ARTICLE INFO

ABSTRACT

On the basis of the unique physical and chemical properties of nanoporous gold (NPG), which was obtained simply by dealloying Ag from Au/Ag alloy, an attempt was made in the present study to develop NPG-based electrochemical biosensors. The NPG-modified glassy carbon electrode (NPG/GCE) exhibited high-electrocatalytic activity toward the oxidation of nicotinamide adenine dinucleotide (NADH) and hydrogen peroxide (H_2O_2), which resulted in a remarkable decrease in the overpotential of NADH and H_2O_2 electro-oxidation when compared with the gold sheet electrode. The high density of edge-plane-like defective sites and large specific surface area of NPG should be responsible for the electrocatalytic behavior. Such electrocatalytic behavior of the NPG/GCE permitted effective low-potential amperometric biosensing of ethanol or glucose via the incorporation of alcohol dehydrogenase (ADH) or glucose oxidase (GOD) within the three-dimensional matrix of NPG. The ADH- and GOD-modified NPG-based biosensors showed good analytical performance for biosensing ethanol and glucose due to the clean, reproducible and uniformly distributed microstructure of NPG. The stabilization effect of NPG on the incorporated enzymes also made the constructed biosensors very stable. After 1 month storage at 4 °C, the ADH- and GOD-based biosensors lost only 5.0% and 4.2% of the original current response. All these indicated that NPG was a promising electrode material for biosensors construction.

© 2009 Elsevier B.V. All rights reserved.

1. Introduction

In recent years, the use of nanostructured materials to construct electrochemical sensors and/or biosensors has aroused the interest of analysts (Manso et al., 2008; Pingarron et al., 2008; Wang, 2005; Wang and Musameh, 2003; Zhou et al., 2008). As far as Au nanoparticles are concerned, the great enhancement in electrochemical response toward nicotinamide adenine dinuclcotide (NADH) and hydrogen peroxide at the Au nanoparticle-modified electrode makes them attractive for the construction of dehydrogenase- and oxidase-based biosensors (Jena and Raj, 2006; Manesh et al., 2008; Pingarron et al., 2008). It is now believed that the excellent catalytic activity of Au nanoparticles relies on the low-coordinated Au atoms, i.e., the atoms on the corners and edges (Hvolbæk et al., 2007).

Nanoporous gold (NPG) is another kind of nanostructured gold. It possesses a three-dimensional spongy morphology with tunable pore and ligament sizes at nanometer scale (Ding et al., 2004; Xu et al., 2007). As compared with Au nanoparticle, NPG has a series of unique characteristics: (1) it is bulk in nature yet nanoscale in microstructure, which means it can be easily applied and recovered; (2) its pore size is tunable in a wide range from a few nanometers to many microns, which facilitates the study on the pore size-dependent effect; (3) prepared by simply dealloying Ag from Ag/Au alloys in concentrated HNO_3, NPG has very clean surfaces, which eliminates the possible poisoning or passivating effects from unwanted molecules or ions such as polymer surfactants and Cl^-, as often used in Au nanoparticle preparation; (4) unlike Au particles, NPG avoids the particle aggregation, thus improving the stability of the NPG-based electrode and prolonging its lifetime.

In addition to its excellent catalytic activity (Xu et al., 2007; Yin et al., 2008; Zhang et al., 2007), NPG was also demonstrated to be a good carrier for biomacromolecule due to its well-ordered pore structure, high-specific surface area and high-specific pore volume (Qiu et al., 2008, 2009; Shulga et al., 2007). Compared with porous silica materials that are electronic semiconductors, NPG is an excellent conductor. Thus, for electrochemical sensors and/or biosensors construction, NPG may have some advantages over Au particles as well as porous silica. In this work, an attempt was made to construct NPG-based electrochemical biosensor. A comparison between the NPG-based biosensors and the gold sheet-based ones was also made to demonstrate the advantages of the NPG as an electrode material.

* Corresponding author. Tel.: +86 531 88365433; fax: +86 531 88365433.
E-mail address: xrhuang@sdu.edu.cn (X. Huang).

2. Experimental

2.1. Reagents

Glucose oxidase (GOD), alcohol dehydrogenase (ADH) and Nafion were purchased from Sigma–Aldrich. NADH and NAD$^+$ were obtained from Bio Basic Inc. Au/Ag alloy (50:50, wt%; 100 nm in thickness) was obtained from Changshu Noble Metal Co. Other chemicals used were of analytical grade. Triply distilled water and 0.1 M PBS (pH 7.2) were used throughout the experiments.

2.2. Apparatus

All electrochemical experiments were performed on a CHI 630C electrochemical workstation (CH Instrument Company, Shanghai, China) at ~25 °C. A three-electrode system was used, including a modified electrode as working electrode, a platinum wire as counter electrode and a saturated calomel electrode (SCE) as reference electrode. All the potentials given in this paper were vs. SCE. The surface morphology of NPG was characterized with a JEOL JSM-6700F field emission scanning electron microscope, equipped with an Oxford INCA x-sight energy-dispersive X-ray spectrometer (EDS) for compositional analysis.

2.3. Preparation of NPG and NPG-based modified electrode

NPG was prepared by dealloying Au/Ag alloy in concentrated HNO$_3$ for 1.5 h, then washing to neutral pH with triply distilled water. The glassy carbon electrode (GCE) was polished to a mirror-like surface with 0.05 μm Al$_2$O$_3$, and then sonicated in water for 5 min. The NPG-modified GCE (NPG/GCE) was made by affixing the NPG leaf to the surface of a GCE (3 mm in diameter).

2.4. Preparation of enzyme electrodes and biosensing of ethanol and glucose

The enzyme loaded NPG/GCE was made by the following procedure: first, a certain amount of an enzyme solution (16 mg mL^{-1}) was coated on NPG/GCE and dried at 4 °C for 5 h, then, to avoid leakage of enzymes, a 2 μL of Nafion (5 wt%) was cast and dried at 4 °C for 5 h. When not in use, the prepared Nafion/ADH-NPG/GCE and Nafion/GOD-NPG/GCE were kept in a refrigerator at 4 °C. Prior to use, they were immersed in 0.1 M PBS (pH 7.2) at ~25 °C for 10 min. The enzyme-modified gold sheet electrode was also made by the same procedure.

The current–time curves for biosensing of ethanol or glucose with the enzyme electrodes were recorded at +0.5 V (ethanol) or +0.4 V (glucose) in 10 mL of stirred PBS (pH 7.2, 0.1 M) containing 3.5 mM NAD$^+$ (for ethanol) or 10 mL of stirred air-saturated PBS (pH 7.2, 0.1 M). An aliquot of ethanol (1.0 M) or glucose (2.0 M) stock solution was injected into the base solution at regular intervals. Each addition increased the concentration of ethanol or glucose by 1.0 mM (ethanol) or 2.0 mM (glucose).

3. Results and discussion

3.1. Characterization of NPG and NPG/GCE

Selective dissolution of silver from Ag/Au alloy results in an open bicontinuous nanoporous microstructure comprised almost entirely of gold. The unusual aspect of the appearance of porosity during dealloying is that the resultant structure is formed dynamically during the etching process. It is not a simple excavation of one phase from a two-phase bicontinuous microstructure. To explain the formation mechanism of the nanoporous structure in the dealloying process, an atomistic model was proposed by Erlebacher et al.
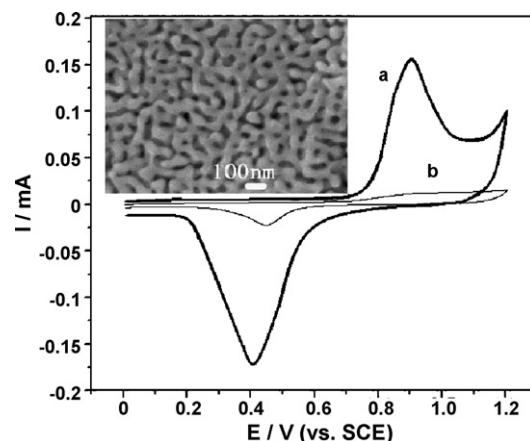

Fig. 1. CVs of NPG/GCE (a) and gold sheet electrode (b) in 0.1 M PBS (pH 7.2). Scan rate: 50 mV s^{-1}. The inset was the SEM image of the NPG with a pore size of ~40 nm.

(2001). This model involves a kind of "interfacial phase separation" in which silver atoms are dissolved and gold atoms left from the alloy/electrolyte interface self-organize and form islands (porosity also forms). Once the porosity forms, due to the extremely fast surface diffusion of gold in an electrolyte, further dealloying still occurs. The dealloying can be easily stopped by simply removing a sample from the etching acid and transferring it to water. The pore/ligament size is thus tunable by changing the etching time. Considering the pore size of NPG, previous results indicated that the catalytic activity of NPG depended on the pore size of NPG. NPG with smaller pore size had relatively higher catalytic activity, but the smaller the pore size, the more unstable the nanoporous structure of NPG especially in acidic environment. The porous structure was more stable when the pore size was larger than 30 nm due to a more complete dissolution of Ag (Yin et al., 2008; Zhang et al., 2007). In addition, a relatively large pore size was necessary for the immobilization of a macromolecule enzyme and for the free access of small molecule substrates and cofactors to the enzyme (Qiu et al., 2008, 2009; Shulga et al., 2007). So, NPG with a pore size of ca. 40 nm was chosen. The inset in Fig. 1 was the SEM image of the NPG sample, which was obtained by dealloying Au/Ag alloy in concentrated HNO$_3$ for 1.5 h. EDS result indicated that Ag atoms in this NPG were almost completely removed. The cyclic voltammograms (CVs) in Fig. 1 showed that the surface of NPG was more active than the good sheet based on the fact that both the oxidation and reduction peaks of the NPG/GCE were negatively shifted as compared with the gold sheet electrode. The CVs of K$_3$[Fe(CN)$_6$] at the two electrodes (see Fig. S-1, Supporting Information) also suggested that the NPG/GCE exhibited a faster electron transfer than the gold sheet electrode (Bard and Faulkner, 1980), because the potential difference (ΔE_p) between the anodic and cathodic peaks at NPG/GCE (80 mV) was much lower than that at the gold sheet electrode (140 mV). All these indicated that NPG was a good candidate as an electrode material for biosensors construction.

3.2. Electrochemical oxidation of NADH and hydrogen peroxide and their detection

The cyclic voltammograms of NADH at both the NPG/GCE and the gold sheet electrode were shown in Fig. 2. At the gold sheet electrode, the electro-oxidation of NADH produced an anodic peak at 0.72 V. At the NPG/GCE, however, the anodic peak occurred at 0.52 V. In addition, the peak current at the NPG/GCE was ca. 2.3 times as high as that at the gold sheet electrode. The marked decrease in overpotential and increase in peak current were obviously resulted from the electrocatalytic activity and the large surface area of NPG.
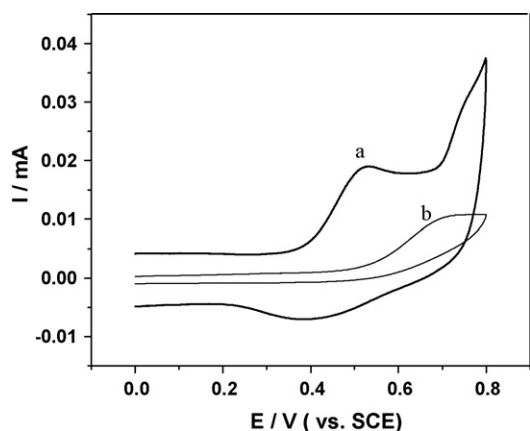
Fig. 2. CVs of NADH (1 mM) at NPG/GCE (a) and gold sheet electrode (b) in 0.1 M PBS (pH 7.2). Scan rate: 50 mV s^{-1}.

Fig. 4. CVs of H$_2$O$_2$ (4 mM) at the NPG/GCE (a) and the gold sheet electrode (b) in 0.1 M PBS (pH 7.2). Scan rate: 50 mV s^{-1}.

As for the catalytic sites of NPG, Hvolbæk et al. argued, based on the density functional calculation, that the activity of a gold catalyst mostly relies on the low-coordinated gold atoms, i.e., the atoms on the corner and edges of gold nanoparticles (Hvolbæk et al., 2007). More recently, Zeis et al. also suggested, based on their investigation on the electrocatalytic reduction of oxygen at NPG, that the active sites of NPG were the gold atoms located in the defect sites (step edges) not those parts of the crystalline surface that contributed to the geometric area (i.e., terraces) (Zeis et al., 2008).

To evaluate the analytical performance of the NPG/GCE, we recorded the amperometric response toward the oxidation of NADH at NPG/GCE (at +0.5 V, the near peak potential at the NPG/GCE, but the onset potential at the gold sheet electrode) with successive addition of 0.1 mM NADH (see Fig. 3). Compared with the gold sheet electrode, the NPG/GCE exhibited wider linear range (0.02–1.0 mM), lower detection limit (9.5 μM) and higher sensitivity (6.9 μA mM^{-1}). In addition, the amperometric response toward NADH at the NPG/GCE was much more stable. For a stirred 0.5 mM NADH solution, the amperometric response at the NPG/GCE at 60 min remained 80% of its initial value; while at the gold sheet electrode, only 40% of the initial value was obtained. This meant that the NPG/GCE had a better resistance to fouling. This feature was very attractive for real applications. Compton et al. reported that at carbon-based electrodes the dense edge-plane-like defective sites on carbon materials had the effect of resistance to fouling (Banks and Compton, 2005). We thought that it was probable that the defective sites on NPG (which were the active sites) might have the same effect. In addition, the improved electron transfer kinet-
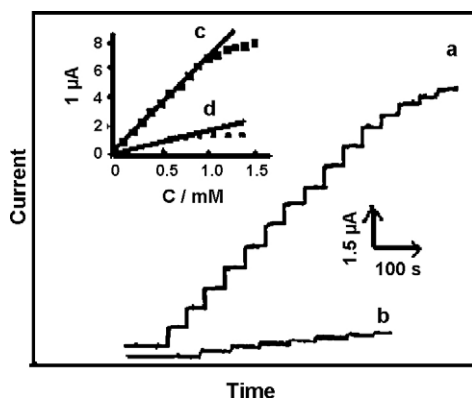
ics of NPG and the free transport of reactants and products in the 3D nanoporous structure of NPG also contributed to the improved signal stability.

The electrochemical behaviors of H$_2$O$_2$ at the NPG/GCE and the gold sheet electrode were shown in Fig. 4. At the NPG/GCE, the oxidation of H$_2$O$_2$ started at ~0.2 V with an oxidation peak at ~0.4 V; at the gold sheet electrode, however, almost no signal was observed. For the reduction of H$_2$O$_2$, at the NPG/GCE, it started at ~0 V with a peak at −0.35 V. At the gold sheet electrode, the reduction started at ~−0.2 V and the signal over the potentials from −0.2 to −0.6 V was very low. All these indicated that NPG exhibited a higher electrocatalytic activity for both oxidation and reduction of H$_2$O$_2$, which, as mentioned earlier, resulted from the unique structure of NPG that had high density of edge-plane-like sites.

Fig. 5 showed the amperometric responses toward H$_2$O$_2$ at the NPG/GCE and the gold sheet electrode upon successive additions of H$_2$O$_2$. For the oxidation of H$_2$O$_2$, the potential was set at +0.4 V (Fig. 5A); for the reduction, the potential was at −0.15 V (Fig. 5B). As shown, the NPG/GCE was very sensitive to the changes in the

Fig. 3. Current–time curves obtained at the NPG/GCE (a) and the gold sheet electrode (b) at +0.5 V upon successive addition of 0.1 mM NADH. Inset: calibration curves for NADH at the NPG/GCE (c) and the gold sheet electrode (d).
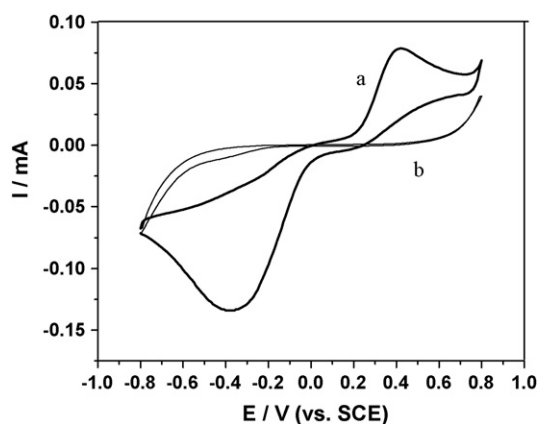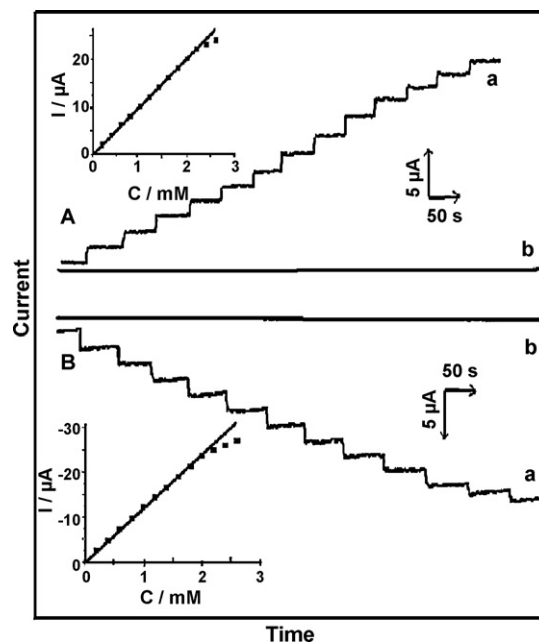

Fig. 5. Current–time curves obtained at the NPG/GCE (a) and the gold sheet electrode (b) at +0.4 V (A) and −0.15 V (B) upon successive addition of 0.2 mM H$_2$O$_2$. Inset: calibration curves for H$_2$O$_2$ at the NPG/GCE at the two potentials.

concentration of H_2O_2 at the two potentials and responded rapidly (within 5 s). However, no obvious responses were observed at the gold sheet electrode. It was concluded that for the sensitive and low-potential amperometric detection of H_2O_2, the NPG/GCE had many advantages over the gold sheet electrode.

3.3. Stability of the NPG/GCE and possible interferences

Like the gold sheet electrode, the NPG/GCE was very stable at room temperature. For 1 mM NADH or 2 mM H_2O_2, no obvious changes in current response were observed after 2 months storage of the NPG/GCE. We also found that 0.2 mM ascorbic acid (AA) or uric acid (UA) did have some interferences to the detection of 1 mM NADH or 2 mM H_2O_2 at the NPG/GCE. Coating a thin Nafion membrane as an effectively permselective barrier on NPG/GCE might eliminate the interferences (Wang et al., 2003).

3.4. Toward biosensing applications based on the electro-oxidation of NADH and H_2O_2

When coupled with alcohol dehydrogenase (ADH) and glucose oxidase (GOD), the NPG/GCE may be used for the sensitive detection of ethanol and glucose based on the high-electrocatalytic activity of NPG for the electro-oxidation of NADH and H_2O_2. NPG was demonstrated to be a good carrier for an enzyme (acetylcholine esterase and laccase) (Qiu et al., 2008, 2009; Shulga et al., 2007). The rationale for the immobilization of an enzyme was based on the spatial confinement of the enzyme to the microstructure of the NPG and the possible interaction between the gold surface and the enzyme via either –NH_2 groups (lysine–gold) or sulfur-containing amino acids on the enzyme (cysteine–gold). Because of the large pore size of the NPG used, when the enzymes interact with the porous surface, the enzymes have enough degrees of freedom to take a preferred orientation. Compared with planar gold for enzymes immobilization, NPG also has the following advantages: (1) its large surface area allows more enzymes to be immobilized, which is important for the rapid response and large signal of an enzyme electrode; (2) its nanoscale porous structure is unfavorable for enzyme leaching; (3) the immobilized enzymes in NPG are more resistant to thermal and time induced denaturalization (Qiu et al., 2008). This stabilization effect is very similar to that observed when porous silica or carbon-based material was used as a carrier for an enzyme immobilization (Sotiropoulou et al., 2005; Vamvakaki and Chaniotakis, 2007).

For the quick conversion of ethanol, the amounts of the loaded ADH and the added its cofactor NAD^+ were separately optimized. For 5 mM ethanol, the amperometric response of the Nafion/ADH-NPG/GCE increased with the increase of the amount of the loaded ADH (from 0.01 to 0.09 mg ADH, [NAD^+] = 2 mM). Higher enzyme loadings were not considered in order to not increasing the biosensor cost. At an ADH loading of 0.09 mg, the current signal increased linearly with the concentration of NAD^+ from 0.2 to 3.5 mM and then leveled off (data not shown). So, 0.09 mg ADH and 3.5 mM NAD^+ were chosen to make the calibration curve for ethanol. As shown in Fig. 6A, the Nafion/ADH-NPG/GCE responded quickly (wthin 10 s) over the studied ethanol concentration range of 1–8 mM. The calibration curve was linear ($R = 0.997$) with a sensitivity of 0.19 $\mu A\,mM^{-1}$ and a detection limit of 120 μM (S/N = 3). AA or UA at a physiological level of 0.2 mM did not show any interference to ethanol detection (2 mM) at pH 7.2 at the Nafion/ADH-NPG/GCE. This should be attributed to the Nafion membrane which acted as an effective permselective barrier (Wang et al., 2003). Our results at Nafion/ADH-NPG/GCE were reproducible. For 2 mM ethanol, the average current signal of five Nafion/ADH-NPG/GCEs (prepared in the same way) was 0.4 μA with a relative standard deviation of 4.5%.
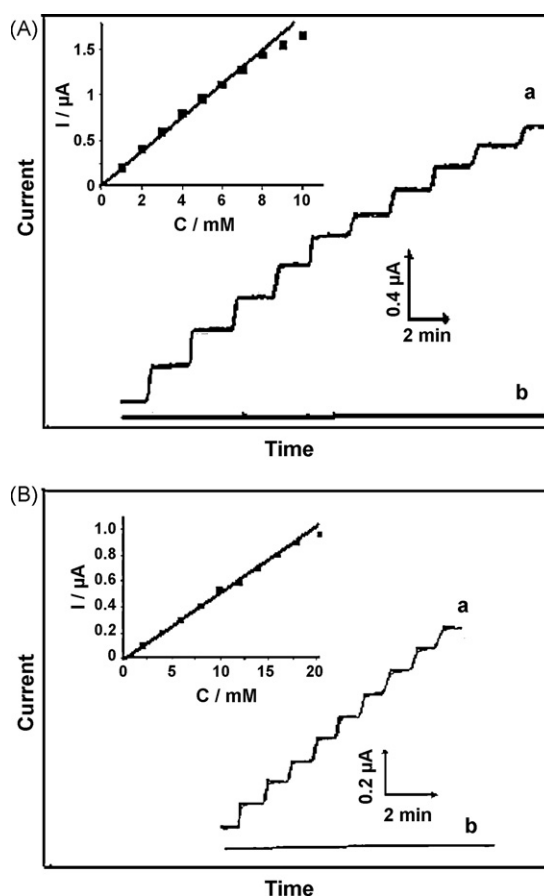

Fig. 6. (A) Current–time curves obtained at Nafion/ADH-NPG/GCE (a) and Nafion/ADH/gold sheet electrode (b) with successive addition of 1 mM ethanol at +0.5 V. Electrolyte: 0.1 M pH 7.2 PBS containing 3.5 mM NAD^+. Inset: calibration curves of ethanol at Nafion/ADH-NPG/GCE. (B) Current–time curves obtained at Nafion/GOD-NPG/GCE (a) and Nafion/GOD/gold sheet electrode (b) with successive addition of 2 mM glucose at +0.4 V. Electrolyte: air-saturated 0.1 M pH 7.2 PBS. Inset: calibration curve of glucose at Nafion/GOD-NPG/GCE.

For the biosensing of glucose, the amount of GOD added was first optimized (the base solution was always air-saturated). For 20 mM glucose, a GOD loading of 0.08 mg was appropriate for the quick conversion of glucose and the fast response of the Nafion/GOD-NPG/GCE to H_2O_2. Fig. 6B displayed the current–time responses of glucose at the Nafion/GOD-NPG/GCE and the Nafion/GOD/gold sheet electrode at pH 7.2 (applied potential +0.4 V). To avoid any possible interference of O_2, a current signal from electro-oxidation (not electro-reduction) of H_2O_2 at high potential was monitored. As shown in Fig. 6B, the Nafion/GOD/gold sheet electrode responded little to each addition of glucose, but the signal at the Nafion/GOD-NPG/GCE electrode was large enough for accurate measurement due to the electrocatalytic activity of NPG toward H_2O_2. The current signal at the Nafion/GOD-NPG/GCE reached a steady state within 10 s. It had a good linear range from 1 to 18 mM ($R = 0.996$) for glucose sensing with a sensitivity of 0.049 $\mu A\,mM^{-1}$ and a detection limit of 196 μM (S/N = 3). Like at the Nafion/ADH-NPG/GCE, the physiological level of AA (0.2 mM) and UA (0.2 mM) only resulted in a negligible amperametric response at the Nafion/GOD-NPG/GCE due to the existence of Nafion membrane which acted as an effective permselective barrier (Wang et al., 2003). All these suggested that the NPG-based biosensor might satisfy the need for the fast and stable detection of plasma glucose (ca. 3–8 mM). In addition, the Nafion/GOD-NPG/GCE was also reproducible. For 5 mM glucose, the average current signal of five Nafion/GOD-NPG/GCEs (prepared in the same way) was 0.28 μA with relative standard deviation of

4.2%. The uniformly distributed pores and ligaments of NPG should be responsible for the good reproducibility.

After 1 month storage at 4 °C, the Nafion/ADH-NPG/GCE and Nafion/GOD-NPG/GCE lost 5.0% and 4.2% current response, respectively. This meant the enzyme-modified NPG-based biosensors were also stable. The good stability of the enzyme electrodes should be attributed to the excellent stability of NPG and the protection (stabilization) effect of its nanoporous structure on the conformation of the enzymes (Qiu et al., 2008). For validation of the accuracy of the present biosensors, two real samples (liquor and glucose injection) were tested and the results obtained using the present biosensors were compared with those obtained using the Chinese pharmacopoeia method. As shown in Table S-1 (Supporting Information), our results were in good agreement with those of the pharmacopoeia method. We also compared the analytical characteristics of the present biosensors with literature data. Due to the widespread use of Au colloid, carbon nanotube and mesoporous carbon in electrochemical sensor design, these material-based electrochemical sensors were chosen for the comparison. The present sensors were comparable to those sensors in terms of linear range, detection limit and sensitivity (Table S-2, Supporting Information). Moreover, the NPG-based biosensors have the following advantages: (1) there is no particle aggregation in NPG, which results in a better stability; (2) NPG is very easy in preparation and handling and no binder is need for the construction of the NPG-based sensors; (3) its clean and reproducible porous structure not only improved the reproducibility and analytical performance of the biosensors but also stabilized the enzymes.

4. Conclusions

In the present study, NPG was used as electrode material for biosensors construction. Compared with the gold sheet electrode, the NPG/GCE exhibited greatly enhanced electrocatalysis toward NADH and H_2O_2, which made the NPG/GCE a sensitive amperometric sensor for the detection of NADH or H_2O_2. When coupled with ADH and GOD, the enzyme-modified NPG-based biosensors were prepared. The Nafion/ADH-NPG/GCE and Nafion/GOD-NPG/GCE exhibited good analytical performance for biosensing ethanol and glucose due to the unique physical and chemical properties of NPG. Compared with mostly used Au nanoparticles, NPG holds some advantages in a way that it can be easily prepared, recovered, and recycled. These may make NPG to be another "popular" material for electrochemical sensors/biosensors construction.

Appendix A. Supplementary data

Supplementary data associated with this article can be found, in the online version, at doi:10.1016/j.bios.2009.03.011.

References

Banks, C.E., Compton, R.G., 2005. Analyst 130, 1232–1239.
Bard, A.J., Faulkner, L.R., 1980. Electrochemical Methods—Fundamental and Applications. John Wiley and Sons, New York.
Ding, Y., Kim, Y.J., Erlebacher, J., 2004. Adv. Mater. 16, 1897–1900.
Erlebacher, J., Aziz, M., Karma, A., 2001. Nature 410, 450–453.
Hvolbæk, B., Janssens, T.V.W., Clausen, B.S., Falsig, H., Christensen, C.H., Nørskov, J.K., 2007. Nanotoday 2, 14–18.
Jena, B.K., Raj, C.R., 2006. Anal. Chem. 78, 6332–6339.
Manesh, K.M., Santhosh, P., Gopalan, A., Lee, K.P., 2008. Talanta 75, 1307–1314.
Manso, J., Mena, M.L., Yanez-Sedeno, P., Pingarron, J.M., 2008. Electrochim. Acta 53, 4007–4012.
Pingarron, J.M., Yanez-Sedeno, P., Gonzalez-Cortes, A., 2008. Electrochim. Acta 53, 5848–5866.
Qiu, H.J., Xu, C.X., Huang, X.R., Ding, Y., Qu, Y.B., Gao, P.J., 2008. J. Phys. Chem. C 112, 14781–14785.
Qiu, H.J., Xu, C.X., Huang, X.R., Ding, Y., Qu Y.B., Gao, P.J., 2009. J. Phys. Chem. C 113, 2521–2525.
Shulga, O.V., Jefferson, K., Khan, A.R., D'Souza, V.T., Liu, J.Y., Demchenko, A.V., Stine, K.J., 2007. Chem. Mater. 19, 3902–3911.
Sotiropoulou, S., Vamvakaki, V., Chaniotakis, N.A., 2005. Biosens. Bioelectron. 20, 1674–1679.
Vamvakaki, V., Chaniotakis, N.A., 2007. Biosens. Bioelectron. 22, 2650–2655.
Wang, J., 2005. Electroanalysis 17, 7–14.
Wang, J., Musameh, M., 2003. Anal. Chem. 75, 2075–2079.
Wang, J., Musameh, M., Lin, Y., 2003. J. Am. Chem. Soc. 125, 2408–2409.
Xu, C.X., Su, J.X., Xu, X.H., Liu, P.P., Zhao, H.J., Tian, F., Ding, Y., 2007. J. Am. Chem. Soc. 129, 42–43.
Yin, H.M., Zhou, C.Q., Xu, C.X., Liu, P.P., Xu, X.H., Ding, Y., 2008. J. Phys. Chem. C 112, 9673–9678.
Zeis, R., Lei, T., Sieradzki, K., Snyder, J., Erlebacher, J., 2008. J. Catal. 253, 132–138.
Zhang, J.T., Liu, P.P., Ma, H.Y., Ding, Y., 2007. J. Phys. Chem. C 111, 10382–10388.
Zhou, M., Shang, L., Li, B.L., Huang, L.J., Dong, S.J., 2008. Biosens. Bioelectron. 24, 442–447.